

Adipose Tissue Remodeling under Ischemia: Death of Adipocytes and Activation of Stem/Progenitor Cells

Hirotaka Suga, M.D.

Hitomi Eto, M.D.

Noriyuki Aoi, M.D.

Harunosuke Kato, M.D.

Jun Araki, M.D.

Kentaro Doi, M.D.

Takuya Higashino, M.D.

Kotaro Yoshimura, M.D.

Tokyo, Japan

Background: Following various types of plastic surgery, such as adipose grafting and flap elevation, adipose tissue undergoes ischemia, leading to hypoxia and nutrient depletion. However, few studies have examined ischemic and/or hypoxic changes in adipose tissue.

Methods: The authors established surgically induced ischemia models by severing blood vessels supplying the inguinal fat pads in mice. The partial pressure of oxygen in adipose tissue was measured with an oxygen monitor, and ischemic changes were analyzed by whole-mount staining, immunohistochemistry, flow cytometry, and Western blotting. The authors also examined cell survival under a hypoxic condition *in vitro*.

Results: Models for three degrees (mild, intermediate, and severe) of ischemia showed approximately 75, 55, and 20 percent of the partial pressure of oxygen level in normal adipose tissue (50.5 ± 1.3 mm Hg), respectively. Adipose tissue atrophy with substantial fibrosis on day 28 was seen, depending on the severity of ischemia. Intermediate and severe ischemia induced elevated expression of hypoxia-inducible factor 1 α and fibroblast growth factor 2 on day 1 and degenerative changes (i.e., apoptosis, necrosis, and macrophage infiltration and phagocytosis) in adipose tissue. Dead cells included adipocytes, vascular endothelial cells, and blood-derived cells, but not adipose-derived stem/progenitor cells. Subsequent to degenerative changes, regenerative changes were seen, including angiogenesis, adipogenesis, and proliferation of cells (adipose-derived stem/progenitor cells, vascular endothelial cells, and blood cells). The authors found that, *in vitro*, the experimentally differentiated adipocytes underwent apoptosis and/or necrosis under severe hypoxia, but adipose-derived stem/progenitor cells remained viable.

Conclusions: Severe ischemia/hypoxia induces degenerative changes in adipose tissue and subsequent adaptive tissue remodeling. Adipocytes die easily under ischemic conditions, whereas adipose-derived stem/progenitor cells are activated and contribute to adipose tissue repair. (*Plast. Reconstr. Surg.* 126: 1911, 2010.)

Various types of plastic surgery, such as fat grafting and flap elevation, result in ischemia and hypoxia of adipose tissue. Vascularization and oxygenation of adipose tissue strongly impact clinical outcomes, such as the long-term volume of reconstructed tissue. Adipose tissue easily degenerates on ischemia, and a significant portion is absorbed after free grafting.^{1–4}

However, most studies have examined ischemic changes in adipose tissue histologically rather than at the cellular and molecular levels. In addition, it is unclear what degree of ischemia or hypoxia induces histologic changes and/or irreversible tissue atrophy in adipose tissue.

Adipose tissue is composed of both adipocytes and other cell types, such as adipose stem/progenitor/stromal cells and vascular endothelial

From the Department of Plastic Surgery, University of Tokyo School of Medicine.

Received for publication January 18, 2010; accepted May 25, 2010.

Copyright ©2010 by the American Society of Plastic Surgeons

DOI: 10.1097/PRS.0b013e3181f4468b

Disclosure: The authors have no conflicts of interest to disclose.

cells.⁵ Each cell type can be distinguished by immunohistochemistry or flow cytometry based on characteristic expression of cell surface markers.⁶ It is estimated that there are 1 million adipocytes, 1 million adipose-derived stem/progenitor cells, 1 million endothelial cells, and 1 to 2 million other cells, such as blood-derived cells, per cubic centimeter of human adipose tissue.^{5,7,8} Adipose-derived stem/progenitor cells play pivotal roles not only in adipose tissue homeostasis^{9,10} but also in adipose wound healing,¹¹ pathogenesis of lipomas¹² and lipedemas,¹³ and increased adipogenesis in obesity.¹⁴ They may also contribute to adaptation of adipose tissue to ischemia. Although many animal models for fat grafting have been reported, none has been able to reproduce the various degrees of ischemia/hypoxia that can occur in adipose tissue.

In this study, we prepared novel animal models of three degrees of adipose tissue ischemia (mild, intermediate, and severe) by modifying our model for ischemia-reperfusion injury of adipose tissue in mice.¹¹ Using these models, we examined the cellular and molecular changes in adipose tissue following surgically induced ischemia, focusing on adipocytes, adipose-derived stem/progenitor cells, and vascular endothelial cells.

MATERIALS AND METHODS

Animal Models

Animals were cared for in accordance with institutional guidelines. Six-week-old ICR mice were anesthetized with pentobarbital (50 mg/kg), and a 2-cm incision was made in the right inguinal region. The subcutaneous inguinal fat pad was exposed together with the nutrient vessels from the femoral vessels and the communicating vessels between the skin and the fat pad. In a sham surgery model, all vessels were left intact. In the mild ischemia model, only the femoral artery was electrocoagulated at a site proximal to the branch to the inguinal fat pad. In the intermediate ischemia model, all communicating vessels between the skin and the fat pad were electrocoagulated. In the severe ischemia model, the femoral artery and all of the communicating vessels were electrocoagulated, permitting only reverse flow from the distal portion of the femoral vessels (Fig. 1). At each time interval, mice were killed, and the right inguinal fat pads were examined with the methods described below. A total of 224 mice were used in this study.

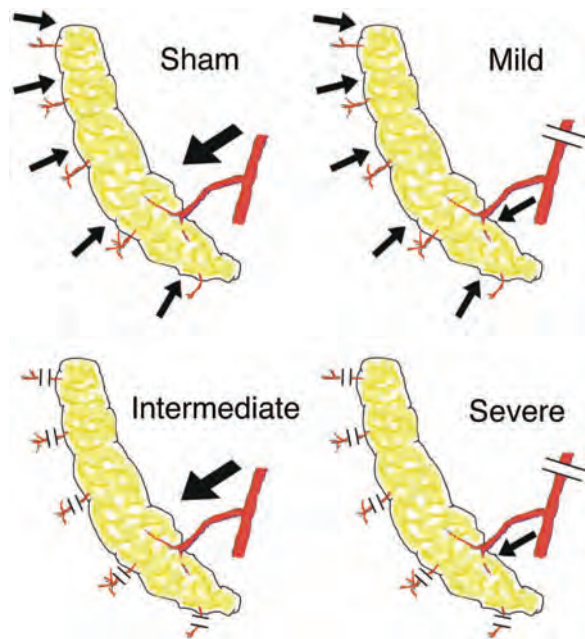


Fig. 1. Three animal models were used for adipose tissue ischemia. Mouse models for three degrees (mild, intermediate, and severe) of ischemia are shown. Ischemia was surgically induced in the inguinal fat pad. The femoral artery in the mild model, the communicating vessels to the skin in intermediate model, and both the femoral artery and communicating vessels in the severe model were electrocoagulated.

Measurement of Partial Pressure of Oxygen in Adipose Tissue

The partial pressure of oxygen (in millimeters of mercury) in adipose tissue was measured with an oxygen electrode (200 μm in diameter) and an oxygen monitor (Eiko Kagaku, Tokyo, Japan). The oxygen electrode was inserted directly into mouse inguinal adipose tissue, and the indifferent electrode was inserted into the abdominal subcutaneous space. The system was allowed to equilibrate for 15 to 20 minutes before every measurement ($n = 8$).

Whole-Mount Staining

Whole-mount staining of fresh adipose tissue was performed as described previously.^{11,14} Briefly, the adipose tissue was minced into 3-mm pieces and incubated with the following reagents for 30 minutes: BODIPY 558/568 or BODIPY-FL (both from Molecular Probes, Eugene, Ore.) to stain adipocytes, Alexa Fluor 488-conjugated isolectin GS-IB₄ (lectin; Molecular Probes) to stain vascular endothelial cells, Hoechst 33342 (Dojindo, Kumamoto, Japan) to stain all nuclei, and propidium iodide (Sigma-Aldrich, St. Louis, Mo.) to stain

nuclei of necrotic cells. The sample was then washed and imaged using a TCS SP2 confocal microscope system (Leica, Heerbrugg, Switzerland). Thirty serial images were obtained at 1- μm intervals and were processed to produce a surface-rendered, 30- μm -thick, three-dimensional image ($n = 3$).

Immunohistochemistry

Harvested adipose tissue was zinc-fixed (Zinc Fixative; BD Biosciences, San Diego, Calif.), paraffin-embedded, and then sectioned at 6 μm for immunostaining using the following primary antibodies: goat anti-CD34 (Santa Cruz Biotechnology, Santa Cruz, Calif.), rabbit anti-Ki67 (Thermo Fisher Scientific, Fremont, Calif.), guinea pig anti-Perilipin (PROGEN, Heidelberg, Germany), and rat anti-MAC-2 (CEDARLANE Laboratories, Burlington, Ontario, Canada) antibodies. Isotypic antibody was used as a negative control for each staining. For visualization with diaminobenzidine, peroxidase-conjugated secondary antibodies appropriate for each primary antibody (Nichirei Biosciences, Tokyo, Japan) were used. Nuclei were counterstained with hematoxylin. For double fluorescence staining, Alexa Fluor 488- or Alexa Fluor 568-conjugated secondary antibodies appropriate for each primary antibody (Molecular Probes) were used. Nuclei were stained with 4',6-diamidino-2-phenylindole. To detect apoptosis, terminal deoxynucleotidyl transferase-mediated dUTP nick end-labeling (TUNEL) staining was performed using the In Situ Cell Death Detection Kit (Roche Diagnostics, Mannheim, Germany) ($n = 3$).

Flow Cytometry

Three and 6 hours before tissue harvest, 5-bromo-2-deoxyuridine was administered intraperitoneally. The adipose tissue was minced into 3-mm pieces, washed with phosphate-buffered saline, and digested on a shaker at 37°C in phosphate-buffered saline containing 0.075% collagenase for 60 minutes. Mature adipocytes and connective tissue were separated from pellets by centrifugation (400 $\times g$ for 5 minutes). The cell pellets (stromal vascular fraction cells) were resuspended, filtered through a 100- μm mesh, and incubated with the following monoclonal antibodies conjugated to fluorochromes for 30 minutes: rat anti-CD31-phycoerythrin (BD Biosciences), rat anti-CD34-fluorescein isothiocyanate (eBioscience, San Diego, Calif.), rat anti-CD45-phycoerythrin Cy7 (Beckman Coulter, Fullerton, Calif.) antibodies, allophycocyanin (APC) 5-bromo-2-deoxyuridine Flow

Kit (BD Biosciences), and Annexin V-APC Apoptosis Detection Kit (BD Biosciences). Cells were then analyzed using an LSR II flow cytometry system (BD Biosciences) ($n = 3$).

Western Blotting

After adipose tissue specimens were homogenized in 1 ml of RIPA lysis buffer (Santa Cruz Biotechnology) and centrifuged, the aqueous layer was collected. Protein concentrations in the samples were determined using the BCA protein assay kit (Pierce, Rockford, Ill.), and equal amounts of protein (10 μg) were loaded in each lane of a gel. The resolved proteins were transferred to a polyvinylidene difluoride membrane (Bio-Rad Laboratories, Hercules, Calif.), and immunostaining was performed using goat anti-fibroblast growth factor (FGF)-2 antibody (R&D Systems, Minneapolis, Minn.), goat anti-hypoxia-inducible factor (HIF)-1 α antibody (Santa Cruz Biotechnology), and goat anti- β -actin antibody (Abcam, Cambridge, Mass.). β -Actin signal served as an internal control. The resulting protein bands were quantified by volume summation of image pixels with Photoshop 7.0 (Adobe Systems, Inc., San Jose, Calif.) ($n = 3$).

In Vitro Cell Death Assay

Mouse adipose-derived stem/progenitor cells were harvested as described previously.¹¹ Cells were cultured in Dulbecco's Modified Eagle Medium supplemented with 10% fetal bovine serum under 6% oxygen, which corresponds to the normal in vivo partial pressure of oxygen. For adipogenic differentiation, cells were exposed to adipogenic medium (Dulbecco's Modified Eagle Medium with 10% fetal bovine serum, 0.5 mM isobutyl-methylxanthine, 1 μM dexamethasone, 10 μM insulin, and 200 μM indomethacin) for 3 days; then, they were maintained in control medium for 10 days. Finally, adipose-derived stem/progenitor cells, and differentiated adipocytes were transferred to a hypoxic condition (1% oxygen), and apoptosis (Annexin V) and necrosis (propidium iodide) were evaluated with a fluorescent microscope. All nuclei were counterstained with Hoechst 33342 (Dojindo) ($n = 4$).

Statistical Analysis

Data are expressed as mean \pm SEM. Comparisons of multiple groups were made using one-way analysis of variance with the Bonferroni multiple *t* test. When the variances of the original data were not equal among groups, the

square root transformation was performed before statistical analysis. Values of $p < 0.05$ were considered statistically significant.

RESULTS

Changes under Mild, Intermediate, and Severe Surgically Induced Ischemia

In our three experimental models, adipose tissue showed varying degrees of hypoxia immediately after surgical induction of ischemia: $37.3 \pm$

2.5 mm Hg in the mild model, $29.2 \pm 1.7 \text{ mm Hg}$ in the intermediate model, and $11.6 \pm 1.0 \text{ mm Hg}$ in the severe model ($n = 8$), compared with $50.5 \pm 1.3 \text{ mm Hg}$ in sham-operated animals (Fig. 2). The decrease in partial pressure of oxygen level gradually recovered over the following 14 days and stabilized. However, on day 28, the partial pressure of oxygen level in the intermediate and severe models remained significantly different from that in the sham model. The weight of adipose tissue

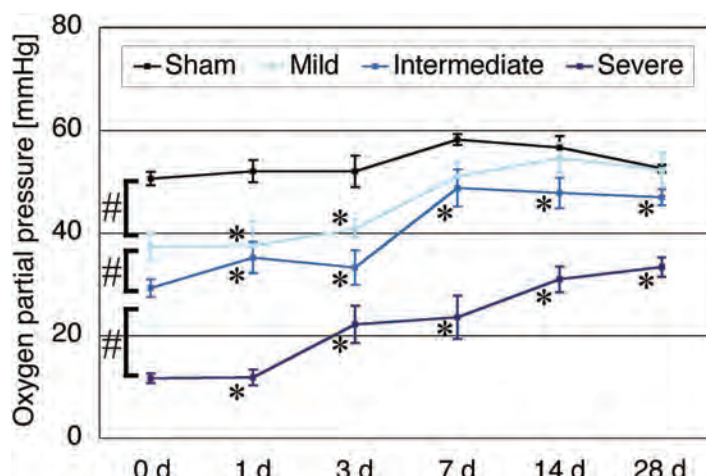


Fig. 2. Partial pressure of oxygen in adipose tissue is shown ($n = 8$ per group). Each hypoxia model showed decreased partial pressure of oxygen, which gradually recovered by day 14. # $p < 0.05$ between indicated groups; * $p < 0.05$ versus sham.

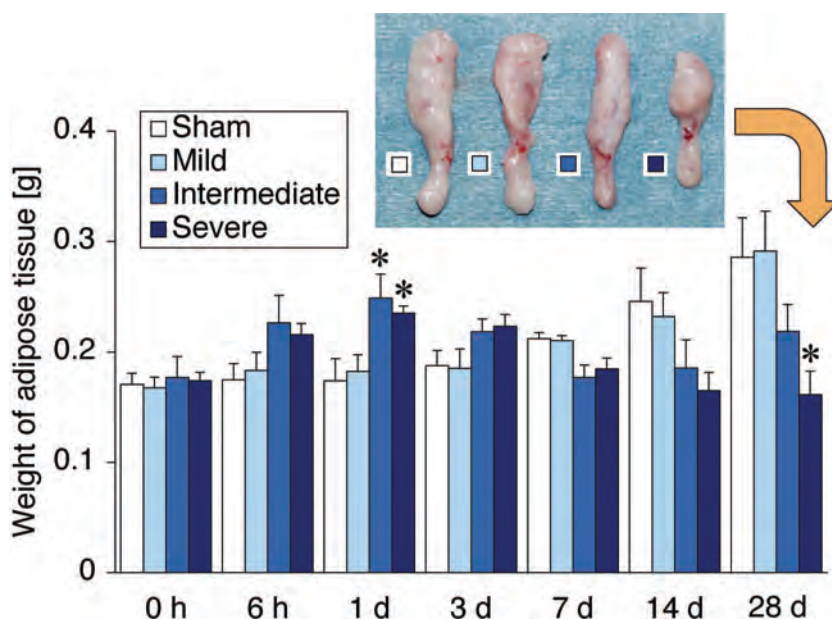


Fig. 3. Weight of adipose tissue at each time point ($n = 5$). A representative sample on day 28 is shown. The weight was significantly lower in the severe model on day 28. * $p < 0.05$ versus sham.

in the intermediate and severe models transiently increased on day 1, suggesting tissue edema (Fig. 3), but was lower than that of controls on day 14. By day 28, the severe model showed a significantly lower mass of adipose tissue than controls, suggesting atrophy of the adipose tissue. This was also evident by macroscopic observation (Fig. 3).

Although there were no histologic changes in the mild model, infiltrating cells and large lipid droplets resulting from adipocyte death were observed in the intermediate model on day 7; however, these changes disappeared by day 28 (Fig. 4). Similar but more marked degenerative changes were observed in the severe model. Furthermore, in intermediate and severe models, small (<50 μm in diameter) adipocytes were frequently observed on days 7 and 14, suggesting that new adipocytes were being generated. Western blotting showed that HIF-1 α and FGF-2 proteins were up-regulated in intermediate and severe models on

day 1, but gradually returned to normal levels by day 28 (Fig. 5).

Degenerative Cellular Events under Severe Ischemia

To further analyze the cellular events during adipose tissue remodeling under ischemia, we examined the severe ischemia model by whole-mount staining, immunohistochemistry, and flow cytometry. TUNEL and propidium iodide staining indicated that apoptosis was most frequently observed on day 1, whereas necrosis occurred predominantly on days 3 and 7 (Fig. 6). There was little apoptosis or necrosis on day 28. Flow cytometry showed that most apoptotic cells (Annexin V-positive) on day 1 were CD45 $^+$ blood-derived cells (83.0 ± 1.8 percent of the total apoptotic cells, $n = 3$) (Fig. 7, left). The CD45 $^-$ population of apoptotic cells consisted mainly of CD31 $^+/-$

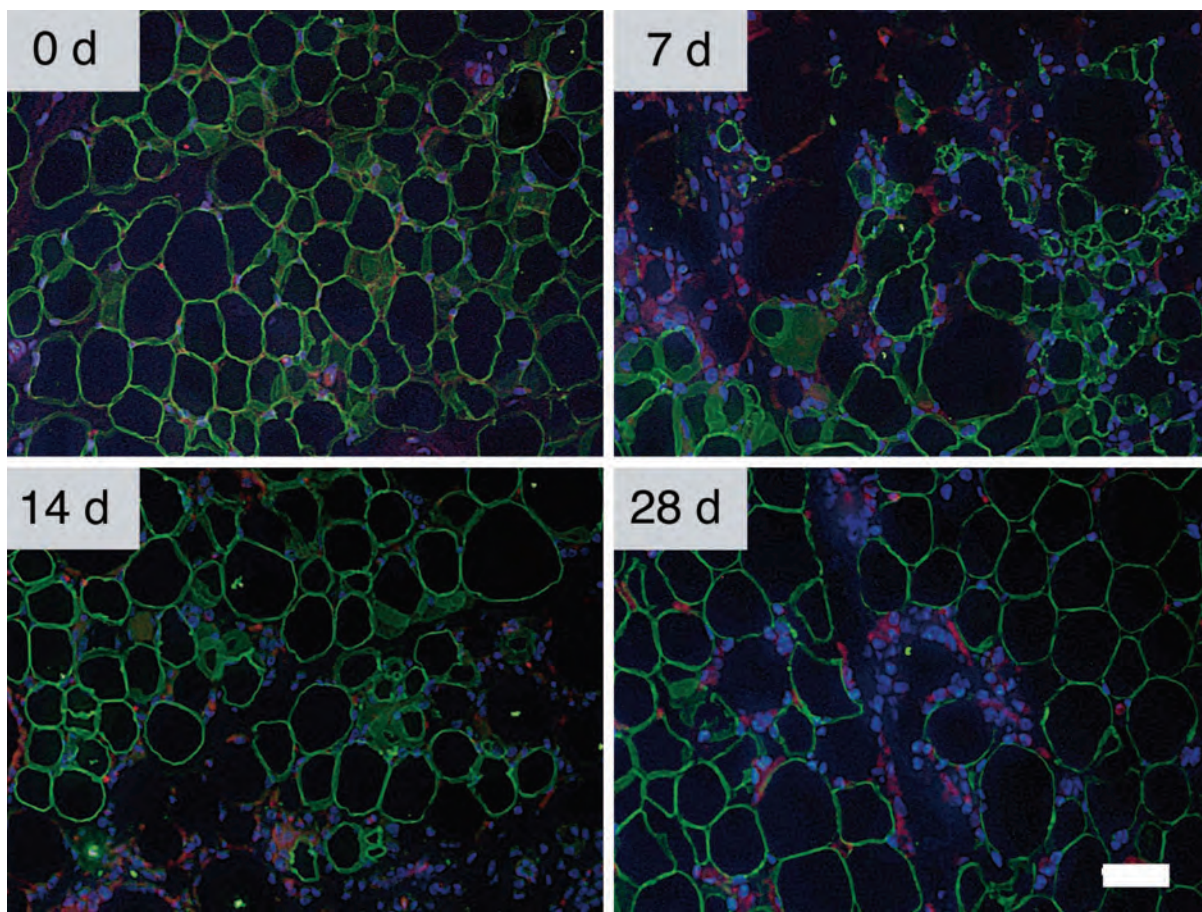


Fig. 4. Sequential microscopic changes in adipose tissue with severe ischemia. Sections were immunostained with perilipin (cell membrane of viable adipocytes, green), lectin (vessels, red), and 4',6-diamidino-2-phenylindole (nuclei, blue). Perilipin-positive small adipocytes and cell infiltration were frequently observed on days 7 and 14. Large lipid droplets resulting from adipocyte death were negative for perilipin. Scale bar = 50 μm .

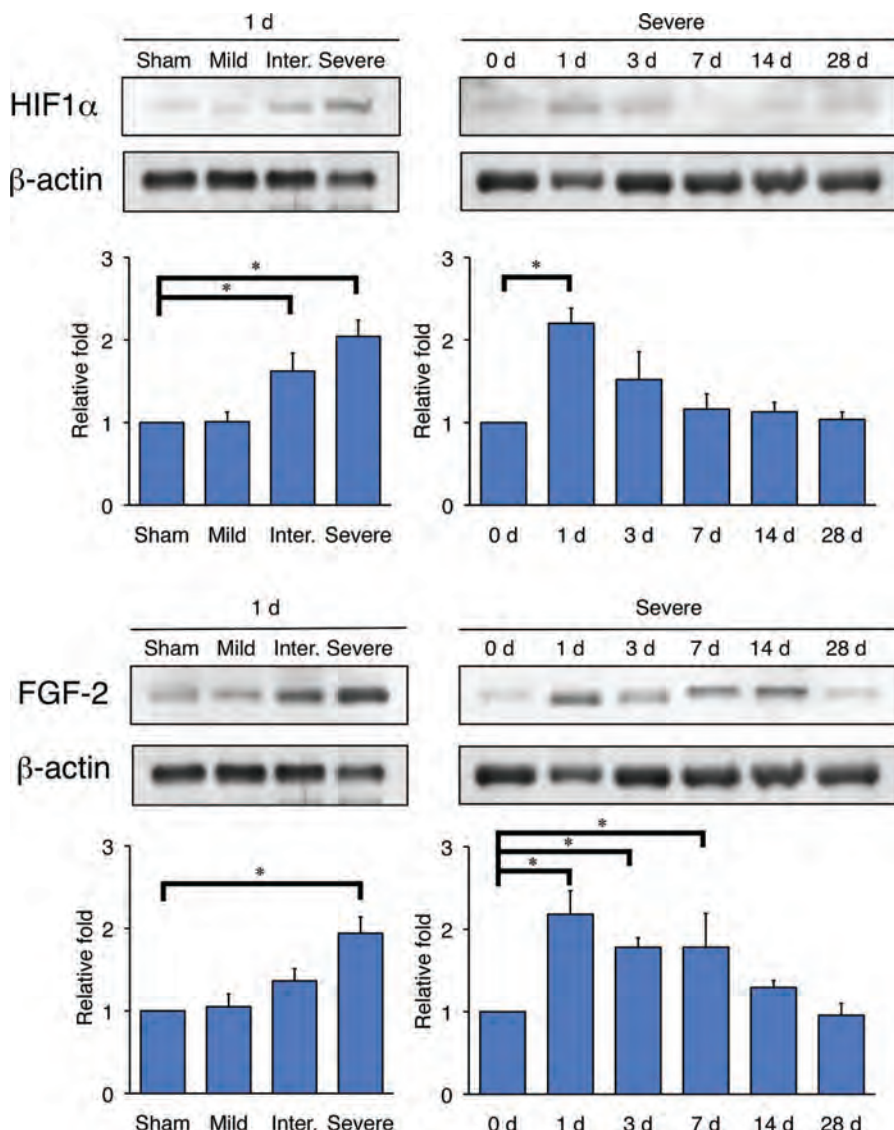


Fig. 5. Expression of HIF-1 α and FGF-2 proteins in adipose tissue with hypoxia. (Above, left) Western blotting for HIF-1 α was performed in each ischemia model on day 1. β -Actin was used as an internal control. HIF-1 α protein was up-regulated in the intermediate and severe models. * $p < 0.05$ versus sham ($n = 3$). Sequential changes in HIF-1 α protein expression in adipose tissue exposed to severe ischemia were observed (above, right). A significant elevation was observed on day 1. * $p < 0.05$ versus day 0 ($n = 3$). (Below, left) Images showing Western blotting for FGF-2 on day 1. FGF-2 protein was up-regulated in the intermediate and severe models. The β -actin signal served as an internal control. * $p < 0.05$ versus sham ($n = 3$). Sequential changes in FGF-2 protein expression in adipose tissue exposed to severe ischemia are shown (below, right). A significant elevation was observed on days 1, 3, and 7. * $p < 0.05$ versus day 0 ($n = 3$).

CD34 $^{+}$ vascular endothelial cells. CD31 $^{-}$ /CD34 $^{+}$ adipose-derived stem/progenitor cells did not undergo apoptosis, suggesting their resistance to ischemia/hypoxia (Fig. 7, right). Whole-mount staining indicated that many adipocytes were dying (propidium iodide-positive) under ischemia on days 3 and 7 (Fig. 8). Recruitment of MAC-2-

positive macrophages was observed from day 3 and peaked on days 7 and 14 (Fig. 9). Interestingly, macrophages accumulated around a perilipin-negative, dead adipocyte, suggesting phagocytosis. A similar “crown-like structure” was reported in obese adipose tissue.^{15–17} Macrophages were sparse even on day 28.

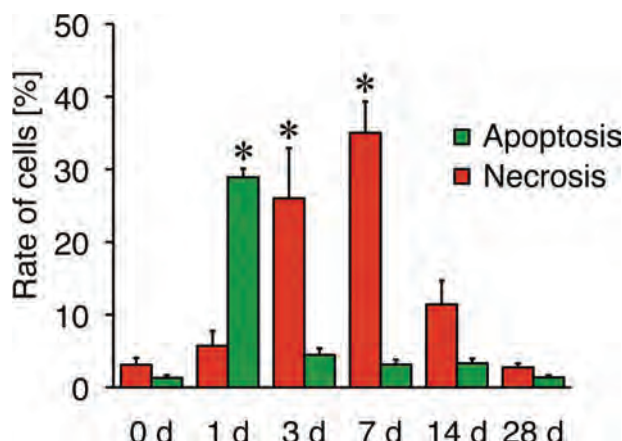


Fig. 6. Analysis of apoptotic and necrotic cells. Number of apoptotic (green) and necrotic (red) cells ($n = 3$). TUNEL-positive apoptotic cells and propidium iodide-positive necrotic cells were counted in histologic sections. Apoptosis was most frequently observed on day 1, whereas necrosis was mostly observed on days 3 and 7. * $p < 0.05$ versus day 0.

Regenerative Cellular Events under Ischemia

The vascular density, which was assessed by the lectin-positive area in whole-mount staining, increased under ischemia on day 7 (Fig. 10, *left*), suggesting that angiogenesis occurs after adipose degeneration induced by severe ischemia. Whole-mount staining also revealed an increase in the number of small adipocytes (<50 μm in diameter) on days 7 and 14 (Fig. 10, *right*, and Fig. 11). These cells were positive for perilipin (a membrane marker for viable adipocytes) and negative for propidium iodide (Figs. 4 and 8), indicating that they were newly generated adipocytes rather than necrotizing adipocytes. Ki67-positive proliferating

cells increased in number under ischemia, peaking on day 7 (Fig. 12, *left*). Immunostaining for Ki67 and CD34 confirmed the existence of Ki67-positive/CD34 $^+$ cells (Fig. 12, *right*), which are likely proliferating adipose-derived stem/progenitor cells or vascular endothelial cells. In addition, flow cytometry of stromal vascular fraction cells revealed that 5-bromo-2-deoxyuridine-positive proliferative cells on day 7 were composed of three populations: CD45 $^+$ blood-derived cells (53.5 ± 9.9 percent of the total proliferative cells, $n = 3$), CD45 $^-$ /CD31 $^+$ /CD34 $^+$ vascular endothelial cells (13.4 ± 1.2 percent), and CD45 $^-$ /CD31 $^-$ /CD34 $^+$ adipose-derived stem/progenitor cells (18.7 ± 2.2 percent) (Fig. 13). These results suggest that ischemia induces adipose tissue remodeling characterized by degeneration (apoptosis and necrosis of adipocytes, vascular endothelial cells, and blood-derived cells) and subsequent regeneration (adipogenesis and angiogenesis), although severe ischemia also induces adipose tissue atrophy and fibrogenesis. In addition, our data suggest that adipose-derived stem/progenitor cells, together with blood-derived cells and vascular endothelial cells, play important roles in the repair process.

In Vitro Cell Death Analysis under Hypoxia

Differentiated adipocytes underwent apoptosis and necrosis as early as 24 hours after they were transferred to the hypoxic condition. Dead adipocytes detached from the dish, and only a few adipocytes remained attached at 72 hours. In contrast, most adipose-derived stem/progenitor cells survived under the hypoxic condition; they did

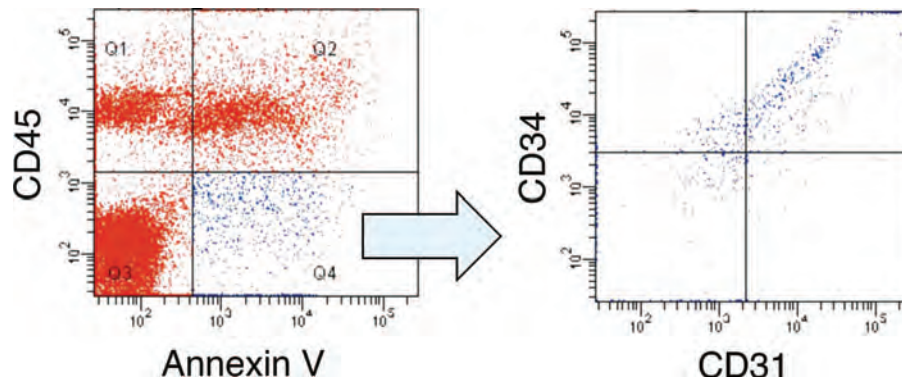


Fig. 7. Flow cytometry of apoptotic cells. Stromal vascular fraction cells were obtained from ischemic adipose tissue on day 1. Most Annexin-positive apoptotic cells were found to be CD45 $^+$ blood cells. Most Annexin-positive/CD45 $^-$ cells were CD31 $^+$ /CD34 $^+$ vascular endothelial cells, and CD31 $^-$ /CD34 $^+$ adipose-derived stem/progenitor cells were not observed among the apoptotic cells.

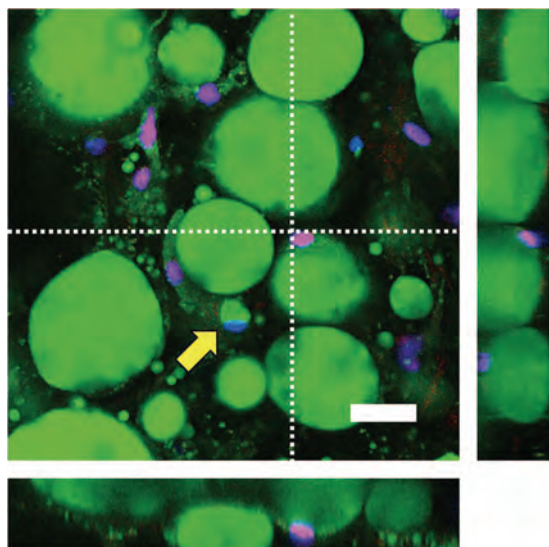


Fig. 8. Histologic analysis of necrotizing adipocytes. Whole-mount staining with BODIPY (adipocytes, green), propidium iodide (nuclei of necrotizing cells, red), and Hoechst 33342 (nuclei, blue) on day 7. Propidium iodide–positive/Hoechst-positive nuclei in necrotic cells are shown in magenta. Horizontal and longitudinal sections at the levels of the white broken lines show a necrotizing adipocyte. A yellow arrow indicates a small adipocyte negative for propidium iodide that is likely a newly generated adipocyte. Scale bar = 25 μ m.

not undergo apoptosis or necrosis even after 72 hours (Fig. 14). The survival rate of adipose-derived stem/progenitor cells was significantly higher than that of differentiated adipocytes in

hypoxia. These results strongly supported the in vivo results described above.

DISCUSSION

In this study, we established novel animal models that reproduce three degrees of ischemia in adipose tissue. Our results demonstrated that irreversible changes in adipose tissue, such as atrophy and scar formation, were induced above a certain threshold of ischemia/hypoxia. The normal partial pressure of oxygen level in mouse adipose tissue was approximately 50 to 60 mm Hg, similar to that reported in humans.¹⁸ Given that intermediate and severe but not mild ischemia induced degenerative changes in adipose tissue, the threshold of tissue oxygenation appears to be between 30 and 35 mm Hg. HIF-1 α , which was up-regulated in the intermediate and severe ischemia models, is known to be a key mediator under hypoxia.¹⁹ Many soluble factors are likely up-regulated through HIF-1 α in ischemic adipose tissue and are involved in the subsequent remodeling of adipose tissue. We also showed that FGF-2 protein expression is significantly elevated only in the severe model. FGF-2 is known to be released from extracellular matrix or dying cells in response to many types of injury without FGF-2 mRNA up-regulation,²⁰ and promotes wound healing by stimulating various cell types, such as adipose-derived stem/progenitor cells.¹¹ Thus, the elevated expression of FGF-2 suggested that severe isch-

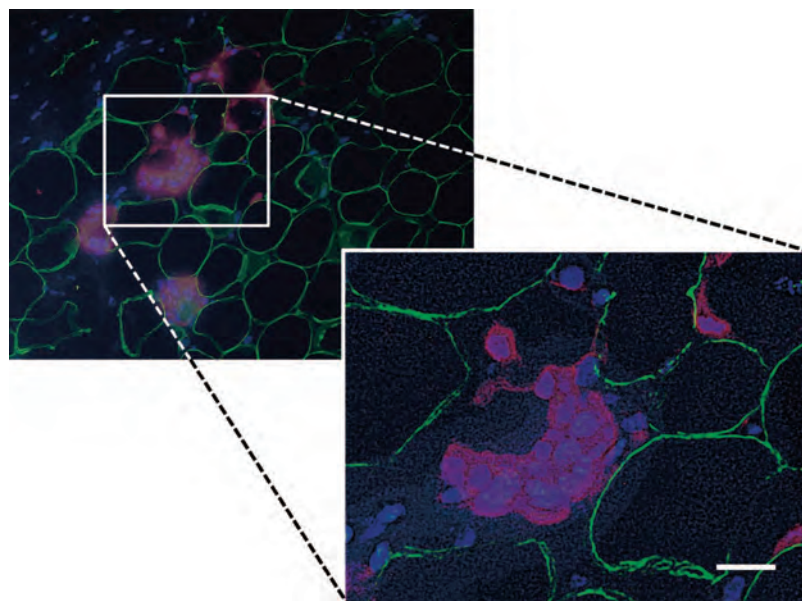


Fig. 9. Immunohistochemistry for MAC-2 (a macrophage marker) on day 28. MAC-2-positive macrophages infiltrated and accumulated around a perlipin-negative necrotic adipocyte. Scale bar = 50 μ m.

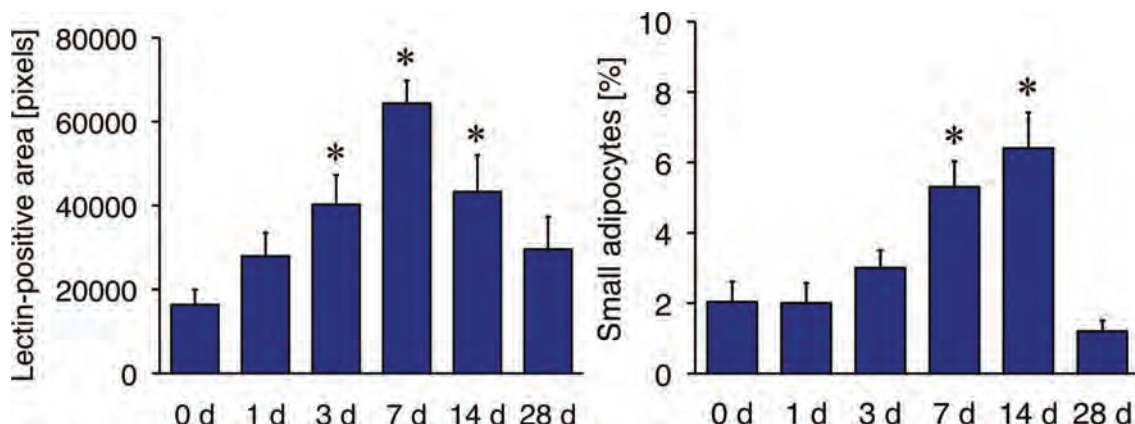


Fig. 10. Regenerative changes in adipose tissue. (Left) Vascular density in whole-mount staining is shown ($n = 3$). The lectin-positive vascular area increased under ischemia, peaking on day 7. * $p < 0.05$ versus day 0. (Right) Bar chart showing the number of small (<50 μm in diameter) adipocytes ($n = 3$). An increased number of small adipocytes was observed on days 7 and 14. * $p < 0.05$ versus day 0.

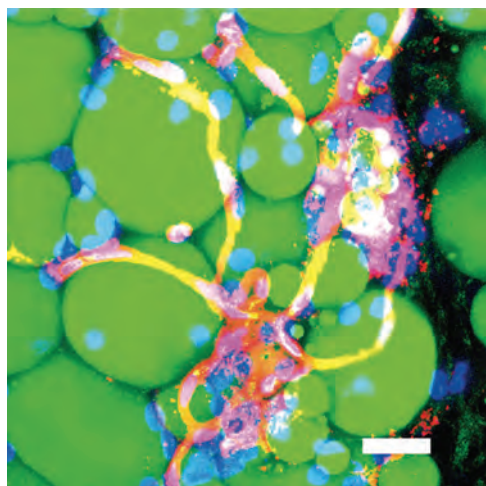


Fig. 11. Whole-mount staining with BODIPY (adipocytes, green), lectin (vessels, red), and Hoechst 33342 (nuclei, blue) on day 14. An increase in vessel density and the number of small adipocytes was observed. Scale bar = 25 μm .

emia may cause substantial injury to the adipose tissue. A recent report suggested that FGF-2 is translationally, but not transcriptionally, up-regulated by hypoxia, and interacts with HIF-1 α .²¹ Further studies are needed to elucidate the detailed mechanisms of FGF-2 expression in ischemic adipose tissue.

This study revealed a series of cellular events in adipose tissue after induction of ischemia. First, severe ischemia induced apoptosis (adipocytes, blood-derived cells, and vascular endothelial cells) on day 1 and necrosis on days 3 and 7. This was followed by macrophage infiltration and phagocytosis. It is interesting that ischemia induces not only degenerative changes but also regenerative

events, characterized by angiogenesis, adipogenesis, and proliferation of cells. This balance between degeneration and regeneration is key for determining the amount of adipocytes, vasculature, scarring, and overall tissue volume.⁵ Fat lysis, partial flap necrosis, deep tissue injury by external forces, and soft-tissue atrophy caused by ischemia are frequently observed clinically. Indeed, any prolonged ischemia/hypoxia (e.g., induced by external pressure and shear, flap elevation, tissue injury, vascular disease, and metabolic disease) would shift the balance toward degeneration, leading to adipose tissue atrophy and fibrogenesis. In contrast, oxygen inhalation or hyperbaric oxygenation elevates the partial pressure of oxygen in adipose tissue above threshold (approximately 60 percent of normal partial pressure of oxygen) and may help to prevent adipocyte death, for example, after lipografting. In fat grafting, transplanted adipose tissue would undergo more severe ischemia/hypoxia than that represented in our models; thus, the balance between degeneration and regeneration would most likely be shifted toward degeneration. Our results strongly suggested that many adipocytes died because of the severe ischemia/hypoxia induced with lipografting and were replaced with new adipocytes derived from resident adipose-derived stem/progenitor cells. Even under the severe ischemia induced with lipografting, our results suggested that adipose-derived stem/progenitor cells survived and contributed to adipose regeneration; however, endothelial cells might not contribute to tissue repair to the extent observed in this study. Based on these observations, we propose that adipose-derived stem/progenitor cell supplementa-

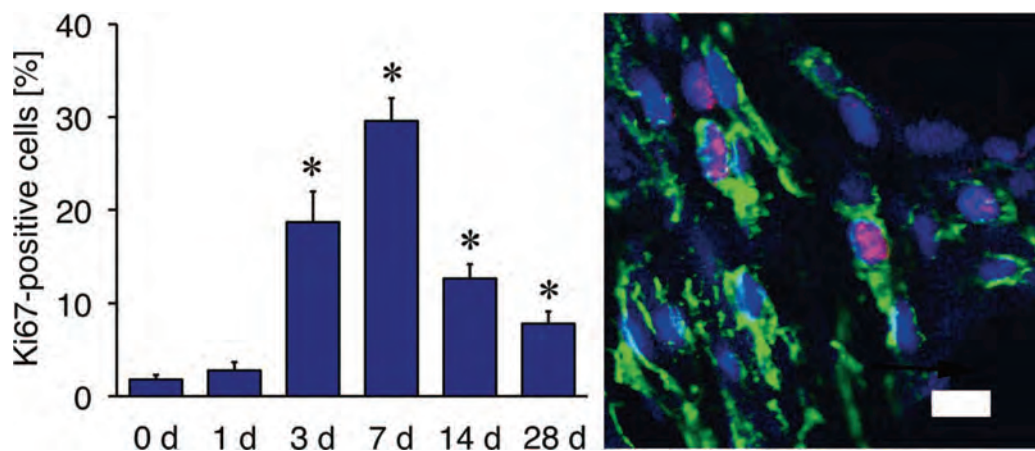


Fig. 12. Analysis of proliferating cells. (Left) Number of Ki67-positive proliferating cells ($n = 3$). Proliferative cells increased in number under ischemia, peaking on day 7. * $p < 0.05$ versus day 0. Immunohistochemistry for CD34 (green), Ki67 (red), and 4',6-diamidino-2-phenylindole staining (nuclei, blue) on day 7 (right). Cells positive for both CD34 and Ki67 were observed. Scale bar = 10 μm .

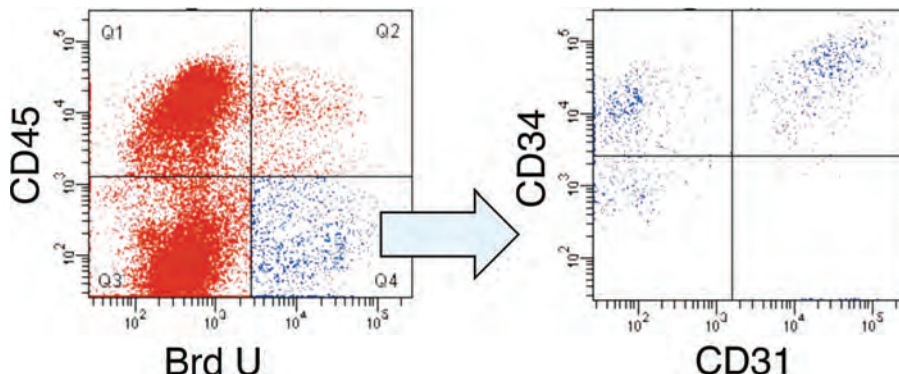


Fig. 13. Flow cytometry of proliferative cells. Stromal vascular fraction cells were obtained from ischemic adipose tissue on day 7. Approximately half of the 5-bromo-2-deoxyuridine-positive proliferating cells were CD45 blood-derived cells. Proliferative adipose-derived (5-bromo-2-deoxyuridine-positive/CD45 $^-$) cells (blue) were found to include both CD31 $^-$ /CD34 $^+$ adipose-derived stem/progenitor cells and CD31 $^+$ /CD34 $^+$ vascular endothelial cells.

tion, which we applied to clinical autologous fat grafting,^{22–25} may augment and accelerate the repair process in adipose tissue under ischemia. Further studies with human adipose tissues are required to elucidate the effects of remodeling and the roles of adipose-derived stem/progenitor cells in free fat grafts.

The newly generated small adipocytes observed in this study suggest that adipogenesis occurs during remodeling after ischemia induction. It is likely that adipose-derived stem/progenitor cells play an important role in this process, but further in vitro studies are needed to test the adipogenic capacity of adipose-derived stem/progenitor cells under ischemia, because some previous

reports have shown that hypoxia impairs adipogenic differentiation,^{26,27} one of the mechanisms that may lead to adipose tissue atrophy in this study. In addition to their adipogenic capacity, adipose-derived stem/progenitor cells have been shown to have proangiogenic capacities. They not only secrete hepatocyte growth factor and vascular endothelial growth factor under hypoxia^{28,29} but also differentiate into vascular endothelial cells,³⁰ though at a low frequency.³¹ It was also shown that adipose-derived stem/progenitor cells have pericytic characteristics and stabilize vascular networks.³² Furthermore, previous studies have shown that adipose-derived stem/progenitor cells could interact with endothelial cells; for example,

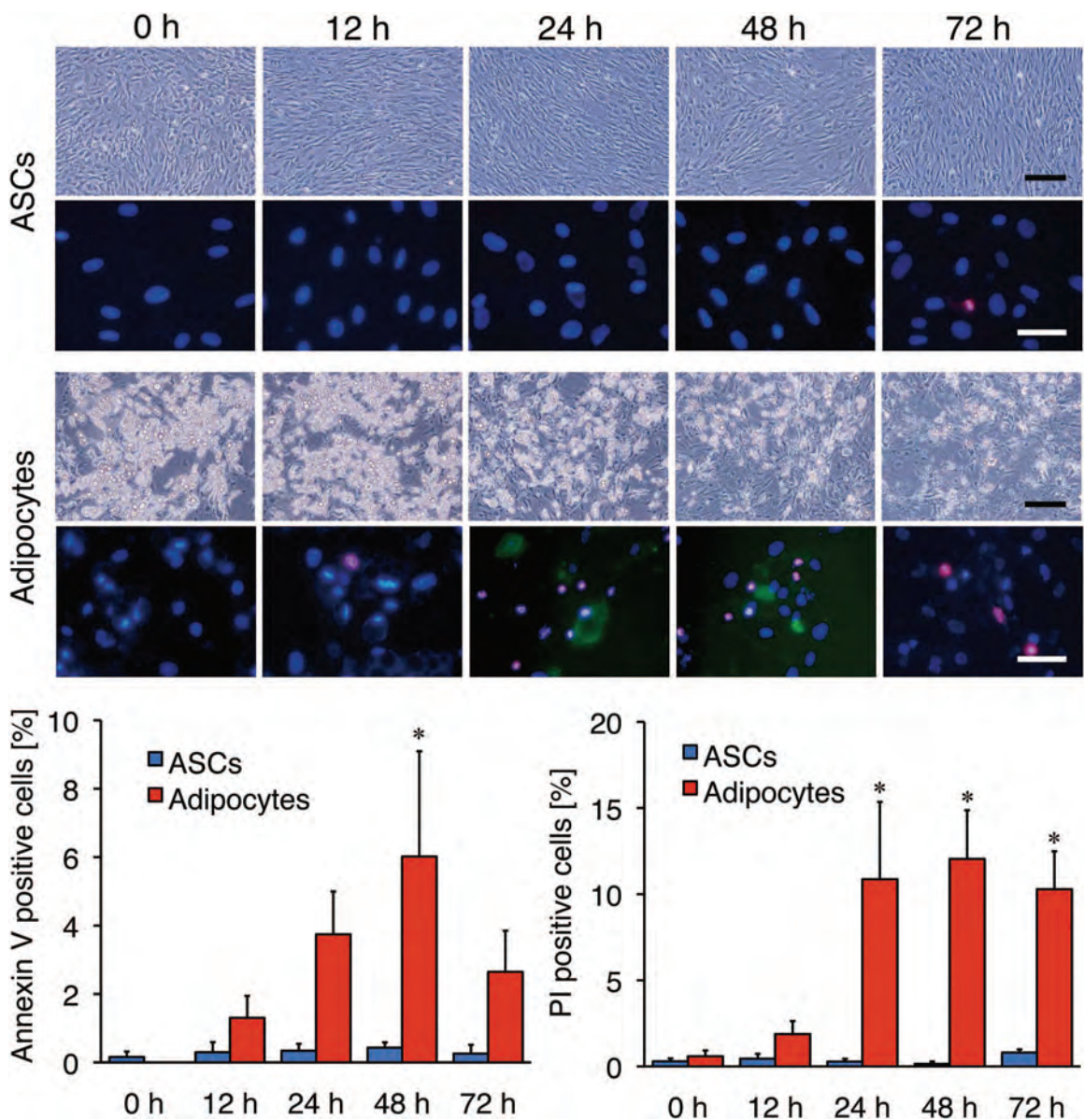


Fig. 14. In vitro cell death assay. (Above) Adipose-derived stem/progenitor cells and differentiated adipocytes were treated under hypoxia (1% oxygen) and stained with Annexin V (green), propidium iodide (red), or Hoechst 33342 (nuclei, blue) at each time point. Differentiated adipocytes underwent apoptosis and necrosis under hypoxia, whereas adipose-derived stem/progenitor cells remained intact. Black scale bars = 200 μ m and white scale bars = 50 μ m. Quantification of Annexin V-positive apoptotic cells (below, left) and propidium iodide-positive necrotic cells (below, right) ($n = 4$) is shown. * $p < 0.05$ versus 0 hour.

conditioned media collected from endothelial cells stimulated adipose-derived stem/progenitor cells,^{32–34} and vice versa.^{28,32} Thus, adipose-derived stem/progenitor cells are likely to contribute to angiogenesis in collaboration with vascular endothelial cells. Although there has been no single marker that specifies adipose-derived stem/progenitor cells, adipose-derived stem/progenitor cells were identified as CD31⁻/CD34⁺ cells in

this study. It is known that adipose-derived stem/progenitor cells do not express CD31 but CD34 and are easily distinguished from vascular endothelial cells, which are positive both for CD31 and CD34. It was also shown that there were few CD31⁻/CD34⁺ cells other than adipose-derived stem/progenitor cells in the adipose tissue,⁶ and this marker combination has been used as a reliable expression profile spec-

ifying adipose-derived stem/progenitor cells in many articles.^{7,8,32,34,35}

Obese adipose tissue is characterized by chronic inflammation, especially accumulation of macrophages around dead adipocytes.^{15–17} Furthermore, recent studies have shown that obese adipose tissue is relatively hypoxic, which may be a basis of adipose dysfunction in obesity leading to insulin resistance and metabolic syndrome.^{18,19,36–38} Unlike lipomas, in which angiogenesis-related genes are up-regulated,¹² a relative decrease in vascular density after adipose enlargement may induce hypoxia in obese adipose tissue. This study showed severe hypoxia with less than half the normal level of oxygenation can induce adipocyte death and subsequent inflammatory reactions such as accumulation of macrophages. Our animal models represent nonobese, nondiabetic adipose tissues. Therefore, they are useful for studying ischemia-induced changes independent of obesity, obesity-associated chronic inflammation, and diabetes-related metabolic factors. In future studies, the model may be useful for elucidating the complex relationship between adipose hypoxia, obesity, and adipose dysfunction.

Mesenchymal stem cells derived from bone marrow were reported to be resistant to exposure to hypoxia; they survive and retain their multipotency under hypoxic conditions.³⁹ We previously showed that adipose-derived stem/progenitor cells escaped apoptosis and play key roles in the repair process after ischemia-reperfusion injury to adipose tissue.¹¹ We previously showed that human adipose-derived stem/progenitor cells remained viable after 1 day of storage at 4°C, but the number of adipose-derived stem/progenitor cells was significantly reduced after more than 2 days of storage.⁴⁰ Here, we showed that in addition to adipose-derived stem/progenitor cells, vascular endothelial cells were detected as a proliferating cell type and appeared to substantially contribute to adipogenesis/angiogenesis in response to ischemia. In contrast, adipocytes and vascular endothelial cells underwent apoptosis after exposure to severe ischemia, whereas adipose-derived stem/progenitor cells escaped from apoptosis. Adipose-derived stem/progenitor cells survived and were activated, contributing to adipogenesis and likely also angiogenesis. These results provide insights into possible therapeutic strategies to avoid or minimize long-term atrophy and scar formation after severe ischemia in adipose tissue. In the future, it would be beneficial to investigate ischemic changes in nonadipose tissues to clarify which changes were specific to adipose tissue.

Kotaro Yoshimura, M.D.

Department of Plastic Surgery
University of Tokyo School of Medicine
7-3-1, Hongo
Bunkyo-Ku, Tokyo 113-8655, Japan
yoshimura-pla@h.u-tokyo.ac.jp

REFERENCES

- Baran CN, Celebioğlu S, Sensöz O, Ulusoy G, Civelek B, Ortak T. The behavior of fat grafts in recipient areas with enhanced vascularity. *Plast Reconstr Surg*. 2002;109:1646–1651.
- Brucker M, Sati S, Spangenberger A, Weinzweig J. Long-term fate of transplanted autologous fat in a novel rabbit facial model. *Plast Reconstr Surg*. 2008;122:749–754.
- Coban YK, Ciralik H. The effects of increased ischemic times on adipose tissue: A histopathologic study using the epigastric flap model in rats. *Aesthetic Plast Surg*. 2007;31:570–573.
- Zhong X, Yan W, He X, Ni Y. Improved fat graft viability by delayed fat flap with ischemic pretreatment. *J Plast Reconstr Aesthet Surg*. 2009;62:526–531.
- Yoshimura K, Suga H, Eto H. Adipose-derived stem/progenitor cells: Roles in adipose tissue remodeling and potential use for soft tissue augmentation. *Regen Med*. 2009;4:265–273.
- Yoshimura K, Shigeura T, Matsumoto D, et al. Characterization of freshly isolated and cultured cells derived from the fatty and fluid portions of liposuction aspirates. *J Cell Physiol*. 2006;208:64–76.
- Suga H, Matsumoto D, Inoue K, et al. Numerical measurement of viable and nonviable adipocytes and other cellular components in aspirated fat tissue. *Plast Reconstr Surg*. 2008;22:103–114.
- Eto H, Suga H, Matsumoto D, et al. Characterization of structure and cellular components of aspirated and excised adipose tissue. *Plast Reconstr Surg*. 2009;124:1087–1097.
- Spalding KL, Arner E, Westermark PO, et al. Dynamics of fat cell turnover in humans. *Nature* 2008;453:783–787.
- Tang W, Zeve D, Suh JM, et al. White fat progenitor cells reside in the adipose vasculature. *Science* 2008;322:583–586.
- Suga H, Eto H, Shigeura T, et al. IFATS collection: Fibroblast growth factor-2-induced hepatocyte growth factor secretion by adipose-derived stromal cells inhibits postinjury fibrogenesis through a c-Jun N-terminal kinase-dependent mechanism. *Stem Cells* 2009;27:238–249.
- Suga H, Eto H, Inoue K, et al. Cellular and molecular features of lipoma tissue: Comparison with normal adipose tissue. *Br J Dermatol*. 2009;161:819–825.
- Suga H, Araki J, Aoi N, et al. Adipose tissue remodeling in lipedema: Adipocyte death and concurrent regeneration. *J Cutan Pathol*. 2009;36:1293–1298.
- Nishimura S, Manabe I, Nagasaki M, et al. Adipogenesis in obesity requires close interplay between differentiating adipocytes, stromal cells, and blood vessels. *Diabetes* 2007;56:901–911.
- Weisberg SP, McCann D, Desai M, Rosenbaum S, Leibel RL, Ferrante AW Jr. Obesity is associated with macrophage accumulation in adipose tissue. *J Clin Invest*. 2003;112:1796–1808.
- Xu H, Barnes GT, Yang Q, et al. Chronic inflammation in fat plays a crucial role in the development of obesity-related insulin resistance. *J Clin Invest*. 2003;112:1821–1830.
- Cinti S, Mitchell G, Barbatelli G, et al. Adipocyte death defines macrophage localization and function in adipose tissue of obese mice and humans. *J Lipid Res*. 2005;46:2347–2355.

18. Pasarica M, Sereda OR, Redman LM, et al. Reduced adipose tissue oxygenation in human obesity: Evidence for rarefaction, macrophage chemotaxis, and inflammation without an angiogenic response. *Diabetes* 2009;58:718–725.
19. Trayhurn P, Wang B, Wood IS. Hypoxia in adipose tissue: A basis for the dysregulation of tissue function in obesity? *Br Nutr*. 2008;100:227–235.
20. Bikfalvi A, Klein S, Pintucci G, Rifkin DB. Biological roles of fibroblast growth factor-2. *Endocr Rev*. 1997;18:26–45.
21. Conte C, Riant E, Toutain C, et al. FGF2 translationally induced by hypoxia is involved in negative and positive feedback loops with HIF-1 alpha. *PLoS One* 2008;3:e3078.
22. Yoshimura K, Sato K, Aoi N, Kurita M, Hirohi T, Harii K. Cell-assisted lipotransfer for cosmetic breast augmentation: Supportive use of adipose-derived stem/stromal cells. *Aesthetic Plast Surg*. 2008;32:48–55.
23. Yoshimura K, Sato K, Aoi N, et al. Cell-assisted lipotransfer for facial lipoatrophy: Efficacy of clinical use of adipose-derived stem cells. *Dermatol Surg*. 2008;34:1178–1185.
24. Yoshimura K, Asano Y, Aoi N, et al. Progenitor-enriched adipose tissue transplantation as rescue for breast implant complications. *Breast J*. 2010;16:169–175.
25. Yoshimura K, Asano Y. Fat injection to the breasts: Cosmetic augmentation, implant replacement, inborn deformity, and reconstruction after mastectomy. In: Hall-Findlay EJ, Evans GRD, eds. *Aesthetic and Reconstructive Surgery of the Breast*. London: Elsevier (in press).
26. Yun Z, Maecker HL, Johnson RS, Giaccia AJ. Inhibition of PPAR gamma 2 gene expression by the HIF-1-regulated gene DECI/Stra13: A mechanism for regulation of adipogenesis by hypoxia. *Dev Cell* 2002;2:331–341.
27. Kim KH, Song MJ, Chung J, Park H, Kim JB. Hypoxia inhibits adipocyte differentiation in a HDAC-independent manner. *Biochem Biophys Res Commun*. 2005;333:1178–1184.
28. Rehman J, Trakhtuev D, Li J, et al. Secretion of angiogenic and antiapoptotic factors by human adipose stromal cells. *Circulation* 2004;109:1292–1298.
29. Thangarajah H, Vial IN, Chang E, et al. IFATS collection: Adipose stromal cells adopt a proangiogenic phenotype under the influence of hypoxia. *Stem Cells* 2009;27:266–274.
30. Planat-Benard V, Silvestre JS, Cousin B, et al. Plasticity of human adipose lineage cells toward endothelial cells: Physiological and therapeutic perspectives. *Circulation* 2004;109:656–663.
31. Nakagami H, Maeda K, Morishita R, et al. Novel autologous cell therapy in ischemic limb disease through growth factor secretion by cultured adipose tissue-derived stromal cells. *Arterioscler Thromb Vasc Biol*. 2005;25:2542–2547.
32. Trakhtuev DO, Merfeld-Clauss S, Li J, et al. A population of multipotent CD34-positive adipose stromal cells share pericyte and mesenchymal surface markers, reside in a periendothelial location, and stabilize endothelial networks. *Circ Res*. 2008;102:77–85.
33. Maumus M, Sengenes C, Decaunes P, et al. Evidence of in situ proliferation of adult adipose tissue-derived progenitor cells: Influence of fat mass microenvironment and growth. *J Clin Endocrinol Metab*. 2008;93:4098–4106.
34. Sengenes C, Miranville A, Maumus M, de Barros S, Busse R, Bouloumie A. Chemotaxis and differentiation of human adipose tissue CD34+/CD31- progenitor cells: Role of stromal derived factor-1 released by adipose tissue capillary endothelial cells. *Stem Cells* 2007;25:2269–2276.
35. Lin G, Garcia M, Ning H, et al. Defining stem and progenitor cells within adipose tissue. *Stem Cells Dev*. 2008;17:1053–1063.
36. Hosogai N, Fukuhara A, Oshima K, et al. Adipose tissue hypoxia in obesity and its impact on adipocytokine dysregulation. *Diabetes* 2007;56:901–911.
37. Ye J, Gao Z, Yin J, He Q. Hypoxia is a potential risk factor for chronic inflammation and adiponectin reduction in adipose tissue of ob/ob and dietary obese mice. *Am J Physiol Endocrinol Metab*. 2007;293:E1118–E1128.
38. Rausch ME, Weisberg S, Vardhana P, Tortoriello DV. Obesity in C57BL/6J mice is characterized by adipose tissue hypoxia and cytotoxic T-cell infiltration. *Int J Obes (Lond.)* 2008;32:451–463.
39. Mylotte LA, Duffy AM, Murphy M, et al. Metabolic flexibility permits mesenchymal stem cell survival in an ischemic environment. *Stem Cells* 2008;26:1325–1336.
40. Matsumoto D, Shigeura T, Sato K, et al. Influences of preservation at various temperatures on liposuction aspirates. *Plast Reconstr Surg*. 2007;120:1510–1517.